

AUTOLYCUS: Exploiting Explainable AI (XAI) for Model Extraction Attacks against White-Box Models

Abdullah Caglar Oksuz
Case Western Reserve University
abdullahcaglar.oksuz@case.edu

Anisa Halimi
IBM Research
anisa.halimi@ibm.com

Erman Ayday
Case Western Reserve University
erman.ayday@case.edu

ABSTRACT

Explainable Artificial Intelligence (XAI) encompasses a range of techniques and procedures aimed at elucidating the decision-making processes of AI models. While XAI is valuable in understanding the reasoning behind AI models, the data used for such revelations poses potential security and privacy vulnerabilities. Existing literature has identified privacy risks targeting machine learning models, including membership inference, model inversion, and model extraction attacks. Depending on the settings and parties involved, such attacks may target either the model itself or the training data used to create the model. We have identified that tools providing XAI can particularly increase the vulnerability of model extraction attacks, which can be a significant issue when the owner of an AI model prefers to provide only black-box access rather than sharing the model parameters and architecture with other parties. To explore this privacy risk, we propose AUTOLYCUS, a model extraction attack that leverages the explanations provided by popular explainable AI tools. We particularly focus on white-box machine learning (ML) models such as decision trees and logistic regression models. These models are widely adapted in many industries due to their simplicity and interpretability. When such models are commercialized, they are considered under black-box settings (i.e., they provide label-only predictions), and the owners of the models aim to keep them private. Thus, under black-box settings, the outcomes received from these models only make sense with explanations. In addition, we focus on the Local Interpretable Model-Agnostic Explanations (LIME) to infer the decision boundaries of white-box ML models and create surrogate models that behave similarly to a target model. We mainly focus on LIME because of its wide adoption, model agnosticism, simplicity, and usability.

We have evaluated the performance of AUTOLYCUS on 5 machine learning datasets, in terms of the surrogate model's accuracy and its similarity to the target model. We observe that the proposed attack is highly effective; it requires up to 60× fewer queries to the target model compared to the state-of-the-art attack, while providing comparable accuracy and similarity. We first validate the performance of the proposed algorithm on decision trees, and then show its performance on logistic regression models as an indicator that the proposed algorithm performs well on white-box ML models in general. Finally, we show that the existing countermeasures remain ineffective for the proposed attack.

1 INTRODUCTION

Machine learning has become a crucial tool for many businesses, enabling them to analyze data and make predictions with greater accuracy and efficiency. To make machine learning accessible to a wider range of businesses, many cloud service providers offer Machine Learning as a Service (MLaaS), providing customers with

pre-trained models and tools to develop and deploy their own models. These services are offered on a subscription or usage-based pricing model, providing customers with cost-effective access to advanced machine learning tools.

As the adoption of MLaaS has grown, so has the need for explainable AI (XAI) [4] tools. These tools are essential for providing customers with transparency and understanding of how decisions are made by the ML models [7]. The lack of interpretability and transparency in models that are inherently black-box or in black-box settings can lead to distrust and reluctance to adopt them. A black-box setting refers to a scenario where the user has limited or no access to the internal workings of a model. Popular XAI techniques like local interpretable model-agnostic explanations (LIME) [37] and SHapley Additive exPlanations (SHAP) [26], aim to address this challenge by providing human-understandable explanations for model predictions. As a result, these techniques are utilized by MLaaS platforms such as Azure Machine Learning [2] and IBM Watson OpenScale [9]. LIME generates local explanations for any machine learning model's individual predictions by creating a new model around the data sample of interest. Whereas, SHAP computes global feature importance values using Shapley values [26] from cooperative game theory [32] and a local approximation of the model to compute feature importance values for the entire dataset.

The monetization of MLaaS and the increasing reliance on the models provided therein have opened up new risks for businesses. One such risk is the threat of inference attacks including membership inference [43], model inversion [15], and model extraction [45]. In particular, the threat of model extraction (or stealing) attacks on MLaaS platforms can result in the theft of proprietary models, valuable intellectual property, and the loss of monetary gains. In such attacks, an adversary attempts to extract a copy of a target machine learning model, either in whole or in part, by training a surrogate model using a set of queries to the target model. In addition, an attacker can potentially execute a model extraction attack more easily using the information provided by XAI tools.

In this work, we propose a novel model extraction attack, AUTOLYCUS, that employs model explanations provided by LIME to generate smarter samples with fewer queries than the state-of-the-art attacks for extracting white-box ML models and their functionality to locally trained surrogate models. We consider LIME because it is a widely adopted AI explanation tool, used by over 3.5k users on GitHub [36], due to its consistency, model agnosticism, simplicity, accessibility, and usability in supervised ML.

AUTOLYCUS is influenced by the line-search retraining method proposed by Tramer et al. [45]. It sends adaptive queries to the vicinity of the decision boundaries of a model, to train a surrogate model later based on those queried samples. However, it differs

from line-search retraining in terms of utilizing explanations. Note that this paper is the closest work to ours. We will describe their attack in Section 6.2 and, compare our work with it in Section 6.3.

In AUTOLYCUS, an attacker generates new data samples to send queries, using the labels and the explanations (i.e., decision boundaries returned by LIME) of the previous queries. By doing so, the queries that the attacker sends are informative, contrary to blind queries like in most label-only attacks [8, 34]. AUTOLYCUS shows how the attacker can efficiently and accurately generate these new data samples and create a surrogate dataset that contains a similar or proportional number of samples per class to the target model. AUTOLYCUS can also draw on information from the samples obtained from other resources. These resources may include previously sampled queries and other datasets.

We demonstrate the effectiveness of the proposed AUTOLYCUS on different ML datasets in terms of the accuracy of the constructed surrogate model and the similarity of the surrogate model to the target one. We show that AUTOLYCUS provides high accuracy and similarity for both decision trees and logistic regression models. Additionally, we demonstrate that AUTOLYCUS outperforms the state-of-the-art and remains effective even in the presence of countermeasures.

Contributions We list the main contributions of the proposed AUTOLYCUS algorithm in the following.

- AUTOLYCUS is an attack with minimal prerequisites with little model knowledge or auxiliary data requirements, making it an easily deployable and efficient solution.
- To the best of our knowledge, AUTOLYCUS is the first model extraction attack that uses AI explanations for specifically targeting white-box models.
- Unlike other existing state-of-the-art methods that rely on exact reconstruction attacks such as Equation-Solving [45], Path-Finding [45], and Lowd-Meek [24], AUTOLYCUS can perform perfect or close-to-perfect reconstructions with fewer queries. It is not constrained by the limitations of the listed attacks, like an all-or-nothing approach or high query budgets, making it more effective in extracting white-box models from black-box settings.
- Since it is not restricted by the all-or-nothing approach of aforementioned attacks, AUTOLYCUS can create budget option surrogate models with comparable accuracy and similarity even when it is under hard query limitations.
- One of the advantages of AUTOLYCUS is its minimal requirements for deployment against the white-box models. With a small auxiliary dataset, its query requirements can be further decreased, making it more efficient and accurate.
- AUTOLYCUS also shows how an attacker can precisely build a shadow dataset (as the surrogate dataset) to launch other inference attacks.
- AUTOLYCUS requires up to $60\times$ fewer queries than Tramer et al.'s state-of-the-art attack against white-box models.

The rest of the paper is organized as follows. In the next section, we go over the related work. In Section 3, we provide some background on XAI. In Section 4, we describe the considered system and threat models. In Section 5, we describe the proposed AUTOLYCUS algorithm in detail. In Section 6, we provide the evaluation results. In Section 7, we show the performance of AUTOLYCUS in

the existence of potential countermeasures. In Section 8, we discuss some extensions and limitations. Finally, in Section 9, we conclude the paper.

2 RELATED WORK

We review two primary lines of related research: (i) privacy attacks in machine learning and (ii) privacy risks due to model explanations. **Privacy attacks in ML.** Research on machine learning privacy has identified several attacks, such as membership inference attacks [8, 23, 39, 43] to determine whether a given user was part of the training dataset, attribute inference attacks [16, 44] to infer additional private attributes of a user based on the observed ones, model inversion attacks [6, 15, 50] to reconstruct data from a training dataset, and model extraction attacks [45] to infer the model parameters/hyperparameters and/or the architecture of a model. In this work, we focus on model extraction attacks where an attacker tries to extract sensitive information or intellectual property from a trained model. The attacker typically has access to the model's input-output behavior and uses this information to build a replica of the model (functionality extraction) [31, 41] or extract other valuable information from it (attribute extraction) [12, 19, 45, 47]. Tramer et al. [45] propose the first model stealing attack considering both white-box and black-box access to ML models. Wang et al. [47] propose a model extraction attack that targets the hyperparameters of ML models. Papernot et al. [34] propose a model extraction attack against black-box DNN classifiers. Such attacks have been shown to be effective against a variety of machine learning models, including decision trees, deep neural networks, and support vector machines [18, 28, 45, 47].

Privacy risk due to model explanations. While XAI techniques are useful for the interpretation of the prediction provided by the machine learning models, they can also be leveraged to enhance privacy attacks. Shokri et al. [42] study the privacy risk due to membership inference attacks based on feature-based model explanations and show how various explanation methods leak information about the training data. Zhao et al. [51] analyze how explanation methods enhance model inversion attacks. Their work focus on image datasets and show that the accuracy of the model inversion attacks increases significantly when explanations are used. Kariyappa et al. [20], Milli et al. [27], Miura et al. [29], Truong et al. [46], and Yan et al. [48] propose various model extraction attacks which exploit AI explanations on black-box image classifiers. Aïvodji et al. [1] utilize counterfactual explanations for model extraction attacks. In this paper, our focus lies on model extraction attacks, in contrast to Shokri and Zhao's work. Furthermore, we investigate white-box models in a black-box setting, while others primarily consider black-box models.

3 BACKGROUND ON EXPLAINABLE AI

Explainable AI (XAI) is an approach for developing artificial intelligence systems that are transparent, interpretable, and can provide clear explanations for their decision-making processes [10, 17]. The goal of XAI is to ensure that AI systems are trustworthy, fair, and accountable, and they can be used to inform human decision-making in a reliable and understandable manner. Traditional AI algorithms like deep learning neural networks can be very effective at making decisions based on large amounts of data, but they are often viewed

as “black boxes” because their internal workings are difficult to understand. This can lead to concerns about bias, discrimination, or errors in decision-making. XAI aims to address these concerns by incorporating methods for transparency and interpretability into the design of AI systems. This may involve using simpler models, providing visualizations or natural language explanations, or detecting anomalous behavior.

In the literature, various XAI techniques have been developed for improving the interpretability and transparency of machine learning models, particularly for neural network models in computer vision. Examples of such techniques include Layer-wise Relevance Propagation (LRP) [3], Deep Taylor Decomposition (DTD) [22], Pattern Difference Analysis (PDA) [52], Testing with Concept Activation Vectors (TCAV) [21], and Explainable Graph Neural Networks (XGNN) [49]. For white-box models such as decision trees, XAI techniques such as Anchors [38], SHAP [26], and LIME [37] can be utilized to provide explanations.

Although the exploitation of AI explanations for adversarial machine learning is a recent area of investigation, there have been several studies that conduct model extraction attacks with XAI guidance on neural networks and image classification tasks. However, there are few studies that target white-box models, especially decision trees, which have fundamental differences from other models and are highly used in daily life due to their simplicity. Thus, exploring the vulnerabilities that AI explanations present to such models, even under black-box settings, represents an uncharted territory and constitutes a valuable contribution to the literature.

This paper aims to leverage LIME explanations for decision tree models under black-box settings where only class labels and some explanations are available. While decision tree models are often considered white-box models that are inherently interpretable, in black-box settings, essential information about their inner workings, such as tree depth, number of leaves, node IDs, and number of samples in each node, is withheld from users due to commercial or privacy concerns. In that sense, LIME is a widely adopted AI explanation tool, used by over 3.5k users on GitHub [36], due to its consistency, model agnosticism, simplicity, accessibility, and usability in supervised ML. In this paper, by exploiting LIME explanations, we aim to enhance the capabilities of model extraction attacks by reducing the average number of queries required.

Local Interpretable Model-Agnostic Explanations (LIME) LIME [37] is a widely used XAI tool that endeavors to provide an understanding of the rationale behind a complex machine learning model’s prediction. This is accomplished by generating a local approximation of the model around a specific instance of interest. To this end, LIME creates a new dataset through perturbation of the instance of interest, executed differently depending on the data type, such as through pixel masking in image data or word replacement in text data. Then, the generated dataset is utilized to produce predictions for each perturbed instance using the original model. Following this, LIME constructs an interpretable model, such as linear regression or decision tree, on the newly generated dataset to explicate the behavior of the original model. The feature weights in the interpretable model denote the relative importance of each feature in the original model’s prediction, presented through means such as a heat-map or feature importance scores. It is important to note that the decision boundaries generated by LIME might not exactly

match the model’s exact decision boundaries due to non-linearity. But, for decision tree models, these local explanations are more accurate and consistent compared to the explanations provided to black-box models.

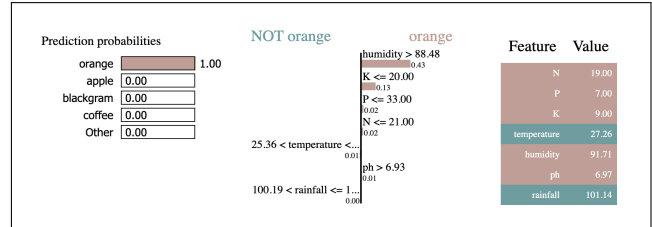


Figure 1: An example LIME explanation from the Crop dataset [30].

We present an illustrative example of LIME applied to a decision tree model trained on the Crop dataset [30]. Figure 1 displays the explanation of an orange sample for this model. On the left-hand side, the prediction probabilities for each class are presented. Note that in decision trees, due to the model’s structure, the prediction probability of a single class is always equal to 1 while the rest is equal to 0. However, in other interpretable models, such as regression models, the prediction probabilities are continuous values ranging from 0 to 1. In the middle section of the figure, the local factors contributing to the model’s decision are listed. These factors are ranked in decreasing order of their explanatory strength. Each local factor is composed of contributing features and their corresponding decision boundary intervals. On the right-hand side, the features and their values are listed, color coded to indicate whether they strengthen or weaken the model’s prediction. This example is intended to demonstrate the functionality of LIME and the type of information it provides for an interpretable model. Further details about the Crop dataset and the experimental setup are presented in Section 6.1 and subsequent sections.

4 SYSTEM AND THREAT MODELS

Consider a target model M that is trained on a dataset D_M and is deployed for use via an API (e.g., in an ML-as-a-Service (MLaaS) platform). Users can send queries to the target model M and receive as an output, the predicted label and the corresponding explanation generated by LIME (as described in Section 3). For instance, a user sends a query for a given sample X_i to the target model M and receives an output including the predicted class y_i , and its corresponding explanations provided by LIME E_i (as shown in Figure 2). A model extraction attack arises when an adversary attempts to learn a surrogate model S that closely approximates M by exploiting both the output of the predicted labels and the explanations returned by LIME. The goal of the attacker is to use as few queries as possible to extract the decision boundaries of M .

We posit that the attacker possesses black-box access to the target model M , including knowledge of its architecture. Notably, the architecture type can be inferred with reasonable accuracy by an individual possessing expertise in machine learning transferability [33]. Furthermore, we assume that the attacker is informed of all possible values that y_i may assume, i.e., the class names, and is thus aware of the total number of classes t . Another assumption we make is that the attacker has access to an auxiliary dataset D_A , comprising multiple samples to initialize the traversal algorithm.

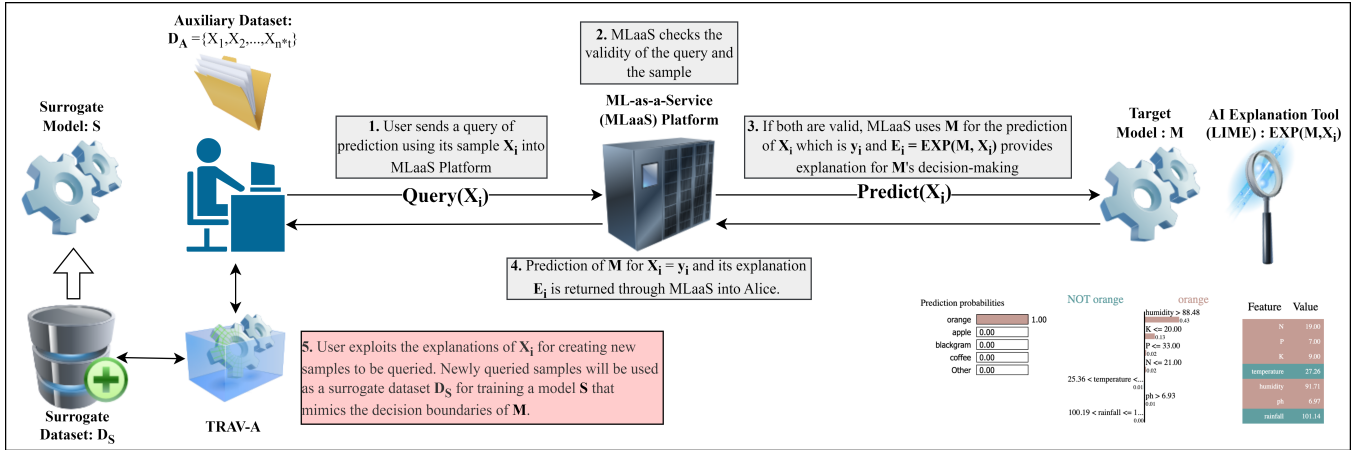


Figure 2: AUTOLYCUS system diagram consisting of the following steps: (1) a user sends a query to the MLaaS platform, (2) the MLaaS platform verifies the validity of the query such that no empty or incomplete queries are sent, (3) the ML model M predicts the class of the queried sample y_i and LIME computes its explanation E_i , (4) the MLaaS platform returns the results to the user, and (5) in case of an adversarial user, they exploit explanations via TRAV-A algorithm to extract the decision boundaries of the target model M .

The composition of D_A may range from a rudimentary collection of samples to comprehensive datasets. In the absence of samples, a random query of default sample values can be utilized to initiate the process. However, it is imperative to note that the exploration capability with such limited samples is inherently restricted, and a higher query budget is necessary for an efficient model extraction attack compared to scenarios where a more extensive D_A is available. In addition, the attacker knows the characteristics of the features of the dataset that is used to train model M , such as their type, domain, and lower and upper bounds.

To promote a clearer comprehension of the symbols and notations that appear frequently in this paper, we direct the reader’s attention to Table 1.

Table 1: Frequently used symbols and notations.

M	Target Model
S	Surrogate Model
D_M	Training dataset of target model
D_S	Training dataset of surrogate model
D_A	Attacker’s auxiliary dataset
D_E	Exploration dataset
Q	Query budget (number of queries)
X_i	Sample i
\hat{X}_i	Altered sample i
x_i^j	Sample i ’s j^{th} feature
\hat{x}_i^j	Altered feature j of sample i
y_i	Predicted class for sample i
E_i	Explanation for sample i
Exp_M	Explainer function of model M
k	Number of top features allowed to be altered
m	Number of total features
n	Number of samples per class
t	Number of total classes
l, u	Lower and upper bounds for the number of samples generated per class
db_i^j	Decision boundaries of the sample i ’s j^{th} feature
δ	Alteration coefficient
TRAV-A	The traversal algorithm

5 PROPOSED WORK

To learn a surrogate model S , that closely approximates the target model M , the attacker first needs to create a surrogate dataset D_S . We assume that the attacker has access to n data samples per class in the auxiliary dataset $D_A = X_1, X_2, \dots, X_{t \times n}$ which may or may not have samples from the original dataset D_M . Here, $X_i = \{x_i^1, x_i^2, \dots, x_i^m\}$, where x_i^j represents the value of feature j in data sample X_i and m is the total number of features. We also assume that there exists a query budget Q which restricts the total number of queries that an attacker can send to the target model M . The proposed model extraction attack is depicted in Figure 2. In Step 1, the attacker sends a query using one of its local samples (from the auxiliary dataset) for generating additional samples. In Step 2, the validity of the query is confirmed. In Step 3, the ML model M predicts the class of the queried sample and LIME computes its explanation. In Step 4, the MLaaS platform returns the results to the user. At the last step (Step 5), the attacker uses the model explanations to generate altered samples that differ from their predecessors by a single feature. This process is informed and guided by explanations, as opposed to sending random queries. As more queries are sent, more samples labeled with the target model’s predictions are retrieved. When these samples are used as training data D_S for surrogate models S , the functionality of the target model is expected to be replicated. In the following, we describe the details of AUTOLYCUS.

5.1 Generating Candidate Data Samples

The goal of the attacker is to send informative queries to the target model M instead of blind queries. For that, the attacker explores the explanations returned by LIME. Assume the attacker sends a query for a given data sample X_i (e.g., one of the data samples in D_A) to the target model M . As discussed, the target model M sends the predicted class y_i , and the corresponding explanation E_i is generated by LIME’s explainer Exp_M for model M . As discussed in Section 3, the explanation returned by LIME consists of the predicted class y_i and the decision boundaries db_i^j ordered by feature importance. Since LIME provides local explanations, the boundaries returned by

LIME do not necessarily reflect the actual decision boundaries of the target model. The same holds for the obtained feature weights.

To generate new and informative candidate data samples, denoted as D_C in Algorithm 1, the attacker considers only the top k features of the data sample X_i . It determines the order of features’ importance by analyzing the “order” of feature weights returned by LIME for the corresponding data sample. The exploration procedure can be likened to a tree search, with the width and depth of the tree depending on the chosen value of k . A higher k value will result in a wider tree with low depth, implying that there are more features, and thus more variants of the same sample that need to be explored. This may lead to the exploration of numerous uninformative samples and ultimately exhaust the query budget. Conversely, a lower k value will yield a slender tree with high depth, indicating that more samples are examined, with only the top features being prioritized. This could result in the inadequate exploration of informative samples, potentially losing crucial information about the structure of the tree. The choice between a high or low value of k as a viable strategy depends on the distribution of feature importance, if known or inferred.

Then, the attacker generates new data samples that differ from the data sample X_i in only one of the top k features. For each of the top k features, it generates candidate samples by analyzing the decision boundaries returned by LIME. The attacker computes the new value of feature j , denoted as \hat{x}_i^j by altering it into the decision boundary db_i^j (returned by LIME) with a small value denoted as δ . Formally, \hat{x}_i^j is computed as:

$$\hat{x}_i^j = db_i^j \pm \delta,$$

where j is the index of the feature that the attacker is aiming to modify and δ is a small alteration factor equal to 1 for categorical features and 0.01 for continuous features. Note that for categorical features, $\delta = 1$ represents the minimum encoding distance whereas for continuous features $\delta = 0.01$ represents the minimum possible distance. The values δ can get ensures that the distance between \hat{X}_i and the decision boundaries is kept minimal. The resulting candidate sample is obtained as

$$\hat{X}_i = \{x_i^1, x_i^2, \dots, \hat{x}_i^j, x_i^m\}.$$

New data samples for the other features are generated, similarly.

Figure 1 shows a toy example of a data sample $X_i = \{19, 7, 9, 27.26, 91.71, 6.97, 101.14\}$ from the Crop dataset [30] and its corresponding explanation. In this example, for $k = 3$, the top features are ‘humidity’, ‘K’, and ‘P’. If we focus on ‘humidity’ and select $\delta = 0.01$, the new generated data sample will be $\hat{X}_i = \{19, 7, 9, 27.26, 88.49, 6.97, 101.14\}$. In cases when LIME returns a more specific decision boundary (e.g., ‘25.36 < temperature < 28.41’), the attacker generates two candidate samples for that feature by exploring both sides of the decision boundary.

5.2 Creating the Surrogate Dataset

In order to have a balanced dataset, the attacker aims at creating a surrogate dataset D_S that contains a similar or proportional number of samples per class to the target model’s training data D_M . This also ensures that the models behave similarly. Thus, it needs to generate a minimum number of samples lower-bounded by a value denoted as l per class and $l \times t$ samples in total. This is to ensure

that no prediction class is under-represented in D_S . In order to use the query budget Q efficiently, the attacker limits the number of samples generated per class to an upper bound value denoted as u . If these bounding values of l and u are not set, more common predicted classes over-populate D_S and hinder the balance of the dataset. Unbalanced D_S causes resulting surrogate models S to over-fit in the common classes and to lose prediction entirely in the rarer classes.

To create the surrogate dataset D_S , the attacker uses the traversal algorithm **TRAV-A**, an algorithm influenced by the line-search retraining algorithm proposed by Tramer et al. [45]. To further elaborate, line search sends adaptive queries to a query oracle, seeking samples in the vicinity of the decision boundaries of a model. The detailed steps are described in Algorithm 1. Recall that the attacker has access to n samples per class from the auxiliary dataset D_A . Thus, initially D_S is limited to D_A . Let D_E denote the dataset with the samples that need to be explored (initially $D_E = D_A$). **TRAV-A** starts by exploring the samples in D_E . It selects the first data sample X_i in dataset D_E and sends a query to the target model M . After receiving the predicted class y_i , **TRAV-A** checks if the maximum number of samples generated for this class has been reached. If that is the case, **TRAV-A** continues by sending a query for the next data sample in D_E , and checking if the above condition is met. Otherwise, **TRAV-A** adds X_i to the surrogate dataset D_S and generates new candidate data samples that differ only on a single feature from the current sample X_i using the explanations provided by LIME. In Section 5.1, we describe how to generate the candidate data samples.

If any of the generated data samples has not been previously explored (i.e., is not a part of D_E), then it is added to D_E . In the next iteration, **TRAV-A** sends a query for the next data sample in D_E . **TRAV-A** employs a breadth-first search strategy to traverse the candidate samples generated during the exploration of a specific sample. We adopt this approach to prevent the deep exploration and propagation of a single sample. This process continues until one of the following conditions is met: (i) there are no unexplored data samples in D_E , (ii) the query budget Q has been exhausted, or (iii) the minimum number of samples l that needs to be generated per class has been reached. Note that the lower bound l should be picked close to the approximate query limit per class Q/t such that the budget is utilized as effectively as possible. It is noteworthy that the last condition (iii) is optional, but it complements the second condition (ii). This condition is included in scenarios where the query budget Q is exceeded without having explored a satisfactory number of samples from each class. Consequently, if the query budget is allowed to be exceeded, condition (iii) can substitute for it and ensure that an adequate number of samples from each class have been examined.

Using the generated surrogate dataset D_S , the attacker trains the surrogate model S . Recall that the attacker knows the architecture of the target model M .

6 EVALUATION

In this section, we describe the datasets, evaluation settings and metrics, and the obtained results.

Algorithm 1 Traversal algorithm used for generating samples that will train the surrogate model

```

1: function TRAV-A( $D_A, M, Exp_M, t, n, l, u, Q$ )
2:    $D_E, D_S, y_S \leftarrow D_A, \{\}, \{\}$ 
3:    $visits \leftarrow \{0, 0, \dots, 0\}$  ▷ (length  $t$ )
4:    $q \leftarrow 0$ 
5:   while  $D_E \neq \emptyset$  and ( $Q \geq q$  or ANY(visits))  $\leq l$  do
6:      $q++$ 
7:      $X_i \leftarrow D_E.POP()$ 
8:      $y_i \leftarrow M.PREDICT(X_i)$ 
9:     if  $visits[y_i] < u$  then
10:       $visits[y_i]++$ 
11:       $D_S.ADD(X_i)$ 
12:       $y_S.ADD(y_i)$ 
13:       $E_i \leftarrow \text{PARSE\_EXP}(X_i, M, Exp_M, t, n)$ 
14:       $D_C \leftarrow \text{GENERATE\_SAMPLES}(X_i, E_i, n)$ 
15:      for  $i$  in  $D_C$  do
16:        if  $i \notin D_E, D_S$  then
17:           $D_E.PUSH(i)$ 
18:   return  $D_S, y_S$ 

```

6.1 Datasets

To evaluate the performance of the proposed algorithm, we employ five widely used datasets of diverse size and complexity, namely Iris [14], Crop [30], German Credit, Breast Cancer, and Adult Income [11] datasets. The Adult Income dataset is utilized in logistic regression experiments whereas the other datasets are utilized in decision tree experiments. For details about the datasets and model properties, please refer to Table 2.

Iris dataset. Iris is a popular dataset [14] used in machine learning for classification tasks. The dataset consist of 4 continuous features such as sepal length, sepal width, petal length, and petal width for three species of Iris flowers. The dataset contains 150 instances (50 instances for each species). It has become a standard benchmark dataset for machine learning algorithms.

Crop dataset. The Crop dataset [30] is a Kaggle dataset used for classification tasks, consisting of continuous variables only. It contains 2200 (100 instances for each crop type) samples from farms in India, with 7 features such as nitrogen, ph, rainfall. The dataset is mainly used to predict the ideal crop type to be raised in the corresponding habitat. In the experiments, we limit the exploratory imbalance caused by the rare crop types by using only 17 crop types.

German Credit dataset. The German Credit dataset (numeric version) [11] contains 1000 credit applications from German banks and credit agencies, with 24 features describing the applicant’s financial history and personal information. Its purpose is to predict the approval of credit applications based on the features. It is commonly used for credit risk modeling, algorithm evaluation, and exploratory data analysis tasks.

Breast Cancer dataset. The Breast Cancer dataset [11] is widely used in machine learning and pattern recognition to describe mass characteristics. It includes 30 features, 10 of which are computed from digitized mass images, and the remaining 20 features are related to the mean, standard error, and worst values of these 10

features. The dataset is labeled with two classes: malignant and benign, making it suitable for binary classification.

Adult Income dataset. The Adult Income dataset [11] contains demographic and employment-related data of individuals sourced from the 1994 U.S. Census database. It includes continuous and categorical features, such as age, education, occupation, and marital status. The goal is to predict the income of an individual, classified as above or below \$50,000. This dataset is commonly used for imbalanced classification tasks.

Table 2: Dataset and model properties.

Dataset	# Samples	# Features (m)	# Classes (t)	Depth	Leaves
Iris	150	4	3	4	8
Crop	1700	7	17	15	32
German Credit	1000	24	2	11	80
Breast Cancer	569	10	2	9	17
Adult Income	48,842	108	2	-	-

6.2 Evaluation Settings and Metrics

Evaluation settings. We use scikit-learn [35] Python package for pre-processing, training, and evaluating the models. Prior to training the models, we apply pre-processing techniques to the datasets by eliminating any missing entries and encoding categorical variables using label encoders, followed by scaling the data using standard input scalers. Each dataset is split into three subsets: (i) the training dataset (75%), (ii) the test dataset (15%), and (iii) the auxiliary set (10%). The training dataset is used to train the target model M , the test dataset to evaluate the performance of the model extraction attacks, and the auxiliary set to create the traversal dataset D_A . The attacker uses D_A as the dataset that starts the traversal algorithm (as described in Section 5.2). We randomly select n samples per class from the auxiliary set to create D_A .

We conduct most of the evaluations on decision trees since other white-box models are prone to easier deterministic extractions and decision trees represent a worst-case scenario. However, we validate the performance of the proposed framework on logistic regression models. The quality of splits in decision trees are measured using the Gini impurity measure [5], which can be different from the measure used to train the target model. Due to the randomness in the training process of decision trees, we train 50 surrogate models on D_S using different random states. We also repeat each experiment 10 times for each auxiliary dataset D_A and report the average of the results.

Evaluation metrics. The experiments aim to evaluate the performance of the constructed surrogate models in comparison to the target models using two distinct metrics. In particular, we employ the accuracy and similarity metrics to measure the efficacy of the constructed surrogate models against the test dataset. Accuracy represents the proportion of correct classifications relative to all predictions made by the surrogate model. In contrast, model similarity gauges the degree of similarity in predictions between the target and surrogate models against the test dataset, regardless of their accuracy. Model similarity is calculated as $1 - R_{test}$, where R_{test} is the average test error or the average distance between predictions over the test dataset. The formal definition of R_{test} , given by Tramer et al. [45], over a test dataset D is $R_{test}(f, \hat{f}) = \sum_{(x,y) \in D} d(f(x), \hat{f}(x)) / |D|$. This measure enables us to determine

the extent to which the generated surrogate models are able to replicate the functionality of the target models.

Comparison with other techniques. We compare the performance of the proposed attack with two other approaches.

Baseline attack. We use the surrogate model S trained on the auxiliary dataset D_A as the baseline attack, where the attacker does not send any queries ($Q = 0$) to the target model. In this scenario, the attacker trains a surrogate model using just D_A as the surrogate dataset D_S .

Tramer attack. Tramer et al. propose a path-finding attack to target decision tree models and an equation-solving attack to target logistic regression models for model extraction [45]. The path-finding attack is an efficient deterministic attack that continues until all the nodes are visited, and eventually, an exact reconstruction is achieved. In [45], the splits in the tree path that a query passes through are exploited by the extraction of node predicates and the creation of alternate samples. Here, node predicate refers to the conditions a sample must satisfy to end up in the same node ID. The alternate samples are generated to explore node IDs outside of node predicates. In the algorithm, the authors use categorical split and line search to deal with categorical and continuous variables, respectively. On the other hand, the equation-solving attack can be employed for logistic regression models and neural networks. This attack converts the query results into linear equations to be solved collectively. Depending on the settings, the extraction may require queries ranging from dozens to hundreds. In the experiments, we use its black-box setup for better comparability. It is important to acknowledge that the path-finding attack targeting decision trees heavily relies on strong assumptions. Retrieving node IDs exposes explicit information about the structure of the model, especially in binary classification tasks, creating a significant vulnerability. Additionally, the allowance of incomplete queries enables a top-down path-finding attack, which is not feasible or realistic in a commercial environment, particularly when starting an attack from the top of the tree. Hence, compared to the path-finding attack, AUTOLYCUS is more applicable in real life. Depending on the architecture of the target model, we use the equation-solving attack for logistic regression or the path-finding attack for decision trees. In the following sections, we refer to any of these attacks as “Tramer attack”.

6.3 Experiments

To assess the effectiveness of AUTOLYCUS, we trained a target model for each of the datasets - Iris, Crop, German Credit, and Breast Cancer datasets are utilized for training decision tree models whereas the Adult Income dataset is used for training a logistic regression model. We study the impact of two parameters on the performance of the proposed attack: (i) the query budget (Q) which is commonly referred to as the maximum number of queries that can be sent to the MLaaS platform, regardless of their utility and (ii) the number of samples per class (n) in the attacker’s auxiliary dataset (D_A). We varied the number of samples per class (n) in D_A (attacker’s auxiliary dataset) from 1 to 5. For each of the datasets, except for the Crop dataset, we compared the number of queries required for the proposed attack to the ones required for the Tramer attack. Tramer et al. [45] did not use the Crop dataset and hence, they did not report the performance on that dataset. The comparison

of results between AUTOLYCUS and Tramer attack is provided in Table 3.

Table 3: Comparison with Tramer attack [45].

Dataset	Tramer attack		AUTOLYCUS	
	$1 - R_{test}$	Queries	$1 - R_{test}$	Queries
Iris	1	644	1	10
German Credit	1	1150	0.64	50
Breast Cancer	1	[644,1150]	0.99	100
Adult Income	1	1485	0.98	100

Figures 3 and 4 show the similarity of the surrogate model to the target model and the accuracy of the surrogate model on the test dataset for varying number of queries for each dataset. For all datasets, we observe that by sending a small number of queries, the proposed attack reaches high similarity and accuracy. We also observe that as the number of queries sent and the number of samples per class (n) known to the attacker increase, the similarity between the target and surrogate models, and the accuracy of the surrogate model increases.

Iris dataset. For the Iris dataset, the attacker obtains a surrogate model S that has a similarity of 1 to the target model M by sending 10 queries to the target model when $n = \{1, 2\}$ (as shown in Figure 3 (a)). For the same setting, the proposed attack provides an accuracy of 0.954 which is identical to the accuracy of the target model (0.954). On the other hand, for the baseline attack ($Q = 0$), the attacker obtains a surrogate model that has a similarity of 0.8 to the target model. This shows that the proposed attack significantly outperforms the baseline approach. The accuracy of models used in Tramer et al.’s study is not provided. But, from the experiments, we can affirm that it is between 0.93 and 1. Thus, we conclude that AUTOLYCUS outperforms Tramer attack as well. More importantly, to achieve a similarity of 1, the proposed attack sends only 10 queries, while Tramer attack requires 644 queries. Thus, by sending at least 60× fewer queries, the proposed attack achieves exact similarity. Notably, the gradual decrease in similarity for $n = \{3, 4, 5\}$ is due to the surrogate models that reach an accuracy of 1 and outperform the target model, which is a phenomenon claimed to be possible to occur in Tramer attack as well.

Crop dataset. In the experiments conducted on the Crop dataset, we observe that the target model has an accuracy of 0.981 with a training dataset of around 1300 samples. Due to having many classes in the Crop dataset, the gradual increase of model similarity is more apparent as the number of queries or the number of samples per class of the auxiliary dataset increases. With $n = 1$, after 1000 queries, similarity and accuracy go up to 0.9. If $n = 5$, a similarity of 0.999 is obtained after sending 1000 queries. Considering the complexity of this model, it is expected that a higher number of queries is required to achieve high accuracy/similarity values. It is worth noting that this dataset employed in the experiments is distinct from the datasets that are used in Tramer attack, and we incorporated it to evaluate the performance of the proposed attack on a complex multi-class prediction model that is more intricate than the multi-class prediction model of the Iris dataset.

German Credit dataset. In the experiments conducted on the German Credit dataset, we observe that the target model has an accuracy of 0.65 with a training dataset of 750 samples. Since this decision tree model does a binary classification with more than 20

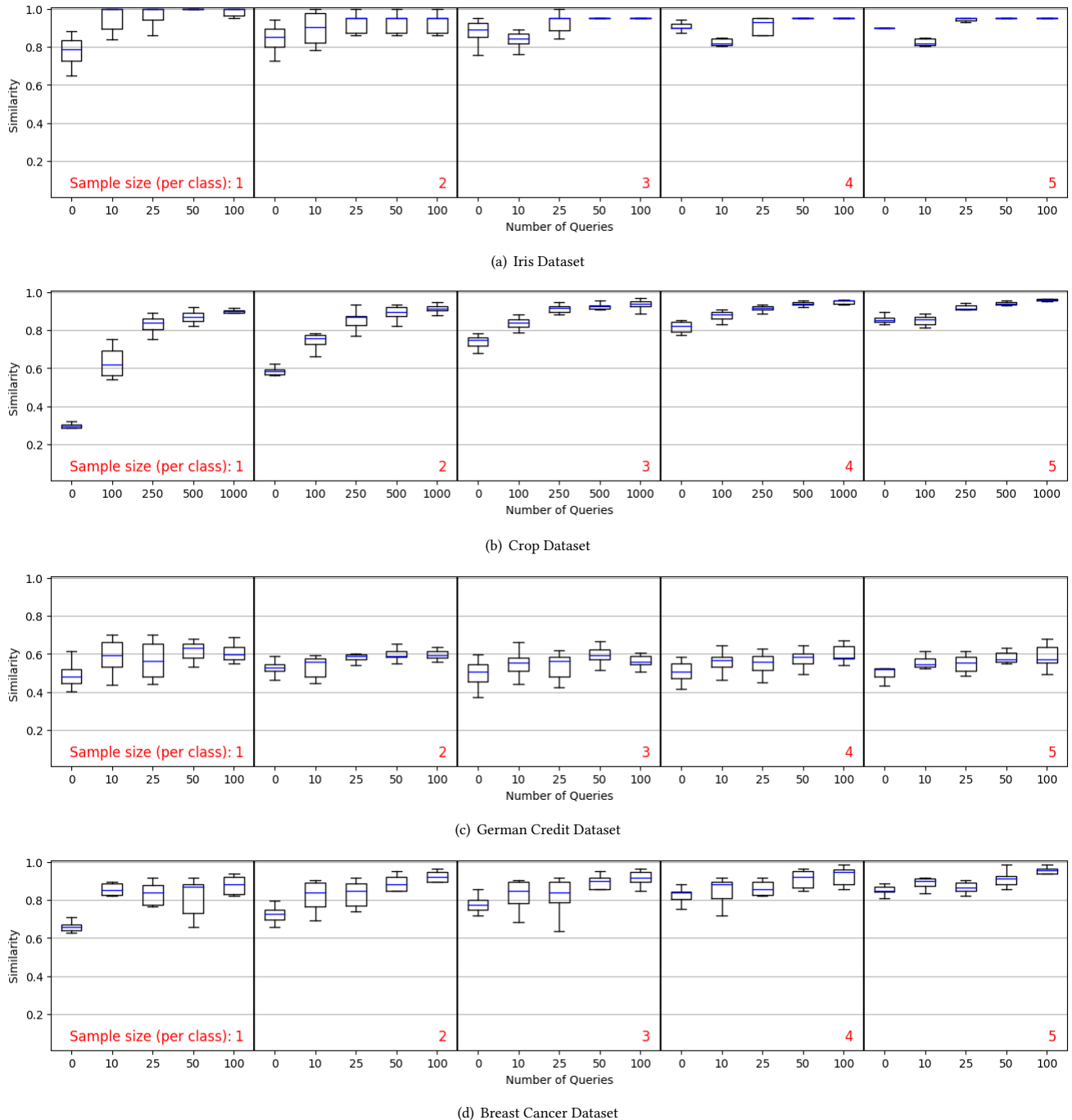


Figure 3: Impact of the number of queries (Q) and D_A 's sample size per class (n) on surrogate model's similarity to target model.

features, it is more prone to over-fitting the target data. Although, surrogate models with accuracies similar to or better than the target model can be achieved with even 10 queries, the samples generated from those queries do not reflect the decision boundaries of the target model and similarity scores remain low for the proposed attack. This is due to a shortcoming of proposed method against the low accuracy models with a high number of influential features (detailed in Section 8). For this dataset, the proposed attack exhibits lower performance than Tramer attack, as Tramer attack was able

to fully extract the target model with 1150 queries in an incomplete query setting. However, it is important to note that this complex tree is extracted by Tramer attack with the available node IDs and top-down approach which significantly simplifies the procedure.

Breast Cancer dataset. We obtain a target model accuracy of 0.94 for the Breast cancer dataset, with a training dataset comprising 420 samples. We observe that the similarity of the model consistently increases as the number of queries increased from 0 to 100. For $n = 5$, implying 10 initial samples, we achieve almost 100%



Figure 4: Impact of the number of queries (Q) and D_A 's sample size per class (n) on the accuracy of the surrogate model.

reconstruction with only 100 queries. Additionally, we are able to obtain comparable surrogate models possessing similar accuracy as the target model with again 10 queries for any $n > 1$, but with lower similarity.

The paper by Tramer et al. does not provide the results of the extraction attack on this dataset. However, based on the performances against the Iris dataset, which results in a simpler model extracted with 644 queries, and the German Credit dataset, which yields a more complex model extracted with 1150 queries, it can

be hypothesized that an ML model trained on the Breast Cancer dataset might be extracted with a number of queries somewhere in between. Notably, the proposed method outperforms Tramer attack by achieving extraction with only 100 queries, which is at least $6.5\times$ less than that of a hypothetical attack.

Attacks against Logistic Regression Models - Adult Income dataset. In the experiments conducted on the Adult Income dataset, the target logistic model achieves an accuracy of 0.802 using a training dataset of 36K samples as shown in Figure 5. We observe

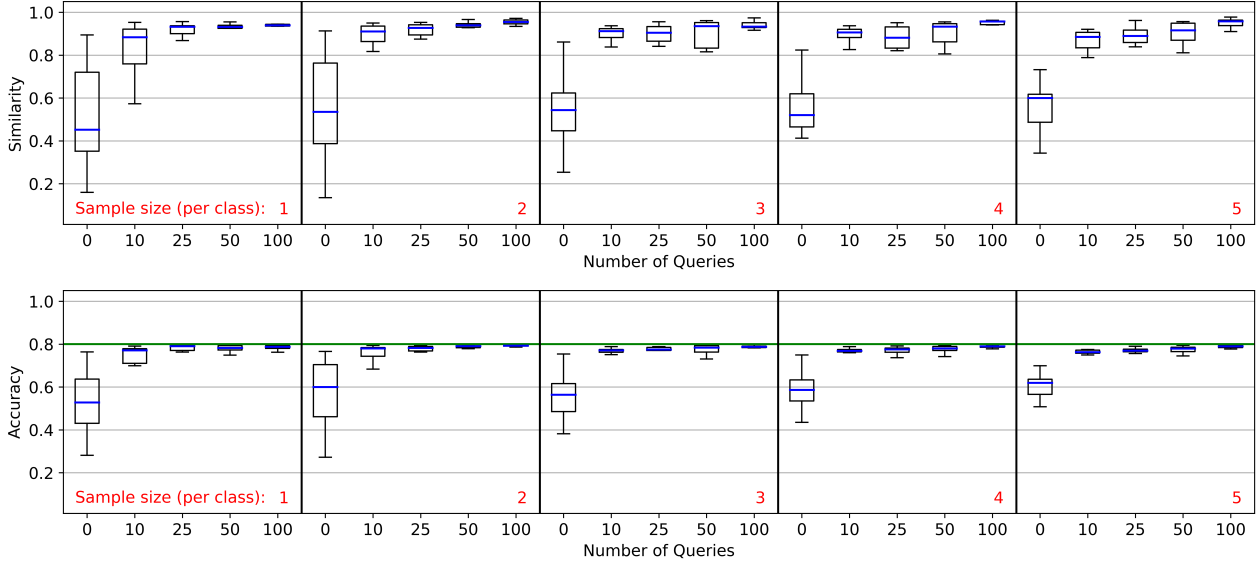


Figure 5: Impact of the number of queries (Q) and D_A 's sample size (per class) (n) on the surrogate model similarity and accuracy for a Logistic Regression Model trained on the Adult Income dataset.

that the baseline attack yields accuracy results varying from 0.3 to 0.77 (0.53 on average) and similarity results varying from 0.16 to 0.9 (0.42 on average). On the other hand, when $n = 1$, the proposed attack generates a surrogate model S with identical accuracy to the target model with only 10 to 25 queries, with a similarity of almost 0.95. For $n = 5$ and $Q = 100$, we obtain models with a similarity of 0.99 to the target model. The proposed method outperforms Tramer attack in this dataset with $15\times$ fewer queries required compared to their 1485 queries and with a 1% similarity difference trade-off.

7 COUNTERMEASURES

In this section, we explore four countermeasures that can be employed against our framework. Two of these are based on differential privacy [13]. These approaches are influenced by Tramer et al.'s suggestions for prediction minimization [45]. While the impact of ensemble methods lies beyond the scope of this paper, as our framework specifically targets white-box models, it is a promising area to explore for future applications on black-box models.

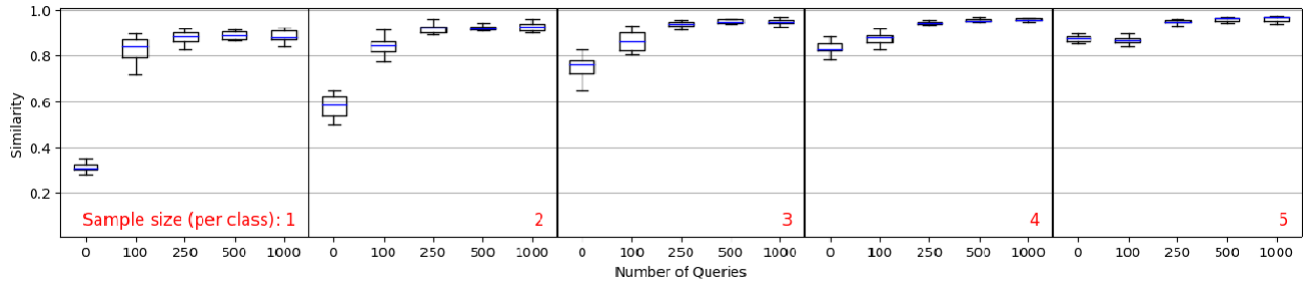
One of the countermeasures explored in our experiments is differential privacy, which serves as a defense mechanism against the model extraction attack. We examine three types of differentially private approaches. The first approach involves the addition of noise to the training data of the target model M . As noted by Tramer et al., this method does not mitigate the model extraction attacks since the objectives do not align, and applying noise may only impede the learning of sensitive information about the training dataset without targeting the boundaries or parameters of models. We verified this by applying naive differential privacy with calibrated Laplacian noise using ϵ values between $[1, \ln(3)]$ to the training data. We observed that this simple application did not effectively mitigate the model extraction attacks and had no significant impact on the decision boundaries. Therefore, as suggested by Tramer et al., we directed our efforts towards targeting the model boundaries.

The second differentially private method we explore is called dynamic distortion. It involves applying noise directly to the decision boundaries of explanations and changing these boundaries as new

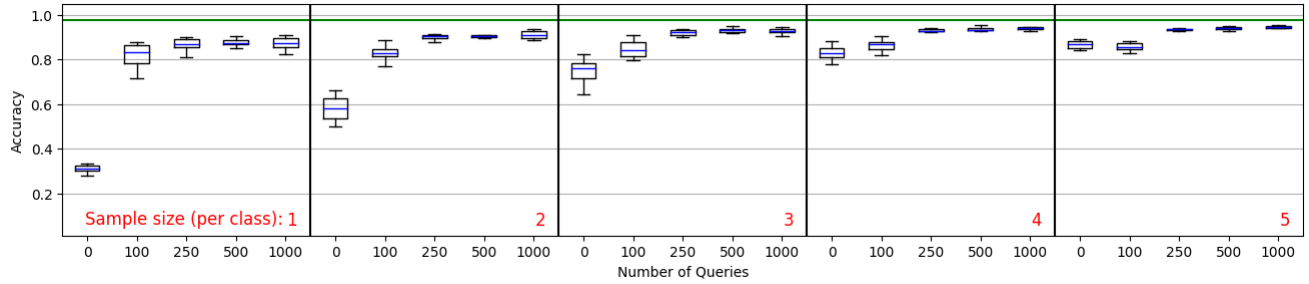
queries are sent to the model. In LIME, the decision boundaries of each feature are static sorted lists, meaning $DB^j = \{db^j_1, db^j_2, \dots\}$ per model, where db^j_i is equal to the neighbors of x_i^j .¹ To implement this countermeasure, we first determined Q queries as our privacy budget and removed Q samples from the training data of the target model. This way for each sample's decision region, we explored how much the decision boundaries of explanations deviate between any neighboring models M and M' . Note that these models are trained with $n * t$ and $n * t - Q$ samples, respectively. Considering a sample X_i and for all neighboring models M and M' , the maximum difference any decision boundary d_i^j can have can formalized as follows: $\sigma_i^j = \max ||M(d_i^j) - M'(d_i^j)||$. Then, we calculated a Laplacian distribution with deviation corresponding to σ as the sensitivity, and for varying ϵ values, we applied Laplacian noise directly to explanation decision boundaries such that they are changed in every query. The results for dynamic distortion when $\epsilon = 1$ are shown in Figures 6 (a) and (b). This method not only fails to mitigate the model extraction attack, but it also enhances the attack strength by allowing a more diverse and informative set of surrogate data to be explored. As demonstrated in the comparison between Figure 3 (b) and, Figure 4 (b) vs. Figure 6 (a) and (b), applying dynamic noise to the boundaries with $\epsilon = 1$ improved the accuracy and similarity results significantly.

The third method is called static distortion method. It's a generic random noise application, using the dynamic distortion approach with $\epsilon = 1$. In this approach though, the noise drawn from the Laplace distribution is unchanged across queries such that the model explanations seem like they are drawn from another model. The results for static distortion are shown in Figure 6 (c) and (d). We observed that this method also fails to mitigate the model extraction attack and, like the previous method, makes the attack even stronger by improving the accuracy and similarity of resulting

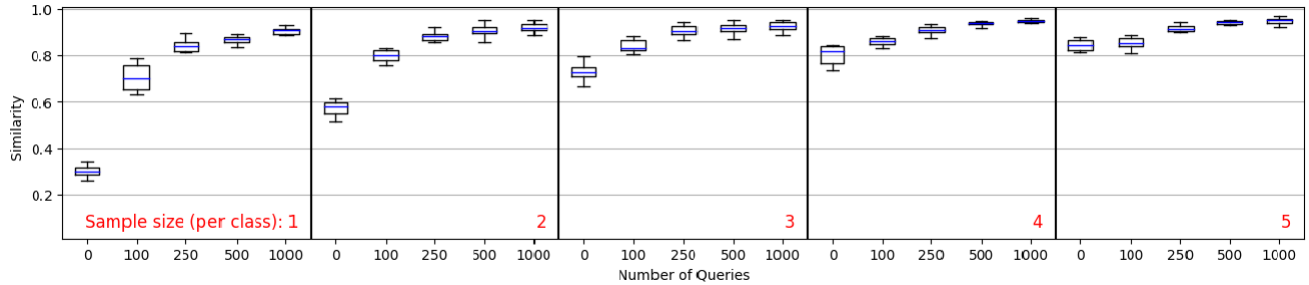
¹Neighboring relationship between the states of features (x_i^j values) is based on the corresponding decision boundaries.



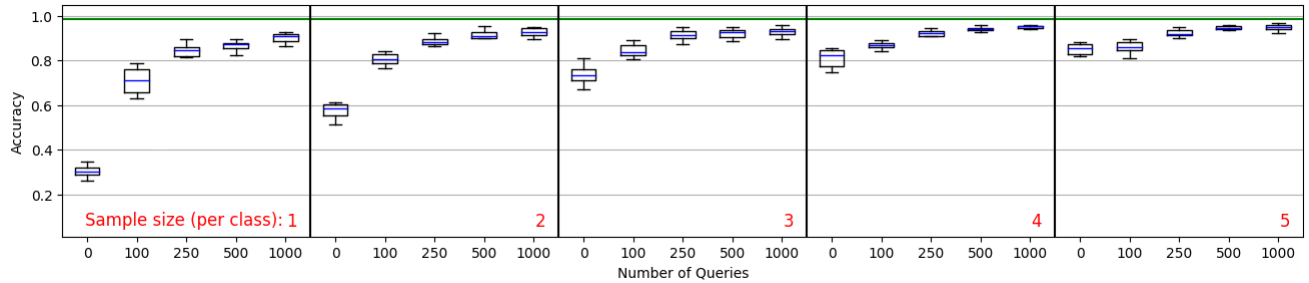
(a) Dynamic Distortion Similarity



(b) Dynamic Distortion Accuracy



(c) Static Distortion Similarity



(d) Static Distortion Accuracy

Figure 6: Impact of countermeasures on the Crop dataset.

surrogate models. However, the improvement in this approach is more negligible compared to the second approach.

In general, we believe that at some point, applying noise with low ϵ values will distort the explanation boundaries (for the dynamic and static distortions) enough to prevent the model extraction attacks. However for such scenarios, the utility of model explanations is expected to be impacted more than the model extraction success.

In our limited experiments with lower ϵ values, the decision boundaries are changed so much that the order of decision boundaries is altered in the sorted list (i.e., LIME output).

Another possible countermeasure suggested by Tramer et al. is rounding the confidence values obtained during predictions. This approach is intuitively effective against models whose information includes confidence values and extraction attacks that deterministically solve boundaries (i.e., equation-solving attacks, path-finding attacks). However, as our method reflects the decision boundaries in

the re-training process stochastically and only employs labels and the decision boundaries of explanations, methods such as rounding confidences or explanation strength do not have any impact on the performance of AUTOLYCUS.

The methods for prediction minimization are prone to failure in our framework, but countermeasures like setting query budgets can slow down the extraction process. Also, alternative procedures like the application of fingerprinting [25] against malicious sharing of surrogate models are not experimented with in this study and they are open for exploration as future work.

8 DISCUSSION

Application to other machine learning models. After obtaining promising results on decision trees, we endeavored to assess the efficacy of AUTOLYCUS against other white-box models in black-box settings. Consequently, our evaluation scrutinized the capabilities of AUTOLYCUS against both decision trees and logistic regression models. Our findings reveal that logistic regression models are more vulnerable to extraction attacks, even with a retraining approach such as AUTOLYCUS, in contrast to commonly used equation-solving methods. Moreover, AUTOLYCUS demonstrates seamless transferability to other models without necessitating any alterations. This discovery implies that AUTOLYCUS can be readily adapted to target other white-box models, with the potential for even superior performance than decision tree models. However, it is yet to be determined whether this attack’s transferability holds for black-box models. Given the explanation inconsistencies in LIME, particularly for black-box model decision boundaries, it poses a challenging task that we consider as future work.

Utilizing other explainability tools. The design preference of using alternative explanation tools in AUTOLYCUS instead of LIME warrants discussion. Two AI explanation tools that work against white-box models, Anchors [38] and SHAP [26], are listed in Section 3. The explanations provided by these platforms must be parsed and transformed into decision boundaries.

Anchors is a method that offers high precision explanations and is a refined successor of LIME. It has the potential to enhance the performance of our attack. However, two issues with Anchors should be considered. Firstly, it is not as widely adopted as LIME, making it less likely to be encountered by MLaaS providers. Secondly, especially for decision trees, the explanations can be overly exact, leaving almost no room for plausible deniability. This characteristic makes it more unrealistic for Anchors to be adapted by commercial MLaaS providers in black-box settings as is. Nonetheless, it can be adapted for models with explanations limited to a small number of features. Such an adaptation aligns with the assumptions we made and can be utilized in AUTOLYCUS.

SHAP utilizes Shapley values [40] of a sample to determine the marginal contribution of each feature. These values are then presented as explanations of that particular sample on a given prediction. However, SHAP is not as straightforward as LIME for identifying the direction of contributing features. It can only be adapted in our method after the transformation of its scalar values into boundaries. The fluctuations in Shapley values can be tested to derive boundaries, using an approach similar to that of Tramer et al.’s line-search algorithm [45]. However, it is yet to be tested.

Overall, we believe that other AI explanation tools like Anchors and SHAP can be utilized in AUTOLYCUS with appropriate modifications in parsing and boundary transformations, similar to LIME. **Limitations.** The primary limitation of our method is the probabilistic reconstruction of models in comparison to the exact reconstruction provided by the attacks proposed by Tramer et al. [45]. Our approach involves retraining models in a black-box setting, and therefore model parameters such as explanations, traversal, or auxiliary datasets are subject to limitations in some models.

For instance, outlier classifications that are not adequately represented in explanations or auxiliary datasets (e.g., outlying branches in decision tree models) may remain undiscovered during the traversal procedure. This limitation is particularly evident in complex models with a high number of influential features, where some branches may not be properly represented in the surrogate model, reducing their similarity to the target model. An example of this limitation was observed in our experiments targeting the German Credit dataset. Despite producing surrogate models with similar accuracy, the low accuracy and multiple influential features of this model made it difficult to adequately discover and functionally represent certain aspects of the model with the assumptions and small auxiliary datasets available to us.

Furthermore, our method’s effectiveness is limited to the type of data that target models are trained on. Our method performs well on tabular data suitable for decision tree models. However, in image classification tasks, LIME explanations of multiple pixels have equivalent strengths, making individually considered features uninformative and rendering our attack useless. Since image classifications consider a collection of pixels or regions in figures, explanations and traversal suited for such a task must be employed. Therefore, AUTOLYCUS should be employed against models with informative LIME explanations.

9 CONCLUSION

In this paper, we have proposed AUTOLYCUS, a novel model extraction attack that exploits the explanations provided by LIME to extract the decision boundaries of white-box models such as decision trees and logistic regression. Our empirical results on five different datasets have shown the effectiveness of the proposed attack. In particular, we have demonstrated that an attacker can exploit LIME explanations to create accurate surrogate models that are highly similar to the target model even under low query budget. We have also shown that the proposed attack requires up to 60× fewer queries than the state-of-the-art attacks while extracting models with similar accuracy and similarity. Furthermore, we have explored potential countermeasures to mitigate this attack such as adding noise to the LIME explanations or adding noise to the training data. Our empirical results have shown that these countermeasures are ineffective for the proposed attack. As future work, we will study the potential increased risk due to explanations in other machine learning models such as neural networks, and work on new and effective countermeasures.

REFERENCES

- [1] Ulrich Aïvodji, Alexandre Bolot, and Sébastien Gambs. 2020. Model extraction from counterfactual explanations. *arXiv preprint arXiv:2009.01884* (2020).
- [2] Microsoft Azure. 2022. Model interpretability - Azure Machine Learning — learn.microsoft.com. <https://learn.microsoft.com/en-us/azure/machine-learning/>

- how-to-machine-learning-interpretability?view=azureml-api-2. (2022). [Accessed 01-May-2023].
- [3] Sebastian Bach, Alexander Binder, Grégoire Montavon, Frederick Klauschen, Klaus-Robert Müller, and Wojciech Samek. 2015. On pixel-wise explanations for non-linear classifier decisions by layer-wise relevance propagation. *PLoS one* 10, 7 (2015), e0130140.
 - [4] Alejandro Barredo Arrieta, Natalia Díaz-Rodríguez, Javier Del Ser, Adrien Benetot, Siham Tabik, Alberto Barbado, Salvador Garcia, Sergio Gil-Lopez, Daniel Molina, Richard Benjamins, Raja Chatila, and Francisco Herrera. 2020. Explainable Artificial Intelligence (XAI): Concepts, taxonomies, opportunities and challenges toward responsible AI. *Information Fusion* 58 (2020), 82–115. <https://doi.org/10.1016/j.inffus.2019.12.012>
 - [5] L. Breiman, J. Friedman, C.J. Stone, and R.A. Olshen. 1984. *Classification and Regression Trees*. Taylor & Francis. <https://books.google.com/books?id=JwQx-WomSyQC>
 - [6] Nicholas Carlini, Chang Liu, Úlfar Erlingsson, Jernej Kos, and Dawn Song. 2019. The Secret Sharer: Evaluating and Testing Unintended Memorization in Neural Networks. In *USENIX Security Symposium*, Vol. 267.
 - [7] IBM Thomas J Watson Research Center. 2019. Explainable Artificial Intelligence (XAI). (2019). <https://www.ibm.com/watson/explainable-ai>
 - [8] Christopher A. Choquette-Choo, Florian Tramer, Nicholas Carlini, and Nicolas Papernot. 2021. Label-Only Membership Inference Attacks. In *Proceedings of the 38th International Conference on Machine Learning (Proceedings of Machine Learning Research)*, Marina Meila and Tong Zhang (Eds.), Vol. 139. PMLR, 1964–1974. <https://proceedings.mlr.press/v139/choquette-choo21a.html>
 - [9] IBM Cloud. 2023. Explaining transactions — ibm.com. <https://www.ibm.com/docs/en/cloud-paks/cp-data/3.5.0?topic=insights-explaining-transactions>. (2023). [Accessed 01-May-2023].
 - [10] Filip Karlo Došilović, Mario Brčić, and Nikica Hlupić. 2018. Explainable artificial intelligence: A survey. In *2018 41st International convention on information and communication technology, electronics and microelectronics (MIPRO)*. IEEE, 0210–0215.
 - [11] Dheeru Dua and Casey Graff. 2017. UCI Machine Learning Repository. (2017). <http://archive.ics.uci.edu/ml>
 - [12] Vasisht Duddu, Debasis Samanta, D Vijay Rao, and Valentina E Balas. 2018. Stealing neural networks via timing side channels. *arXiv preprint arXiv:1812.11720* (2018).
 - [13] Cynthia Dwork, Frank McSherry, Kobbi Nissim, and Adam Smith. 2006. Calibrating noise to sensitivity in private data analysis. In *Theory of Cryptography: Third Theory of Cryptography Conference, TCC 2006, New York, NY, USA, March 4-7, 2006. Proceedings 3*. Springer, 265–284.
 - [14] R. A. FISHER. 1936. THE USE OF MULTIPLE MEASUREMENTS IN TAXONOMIC PROBLEMS. *Annals of Eugenics* 7, 2 (1936), 179–188. <https://doi.org/10.1111/j.1469-1809.1936.tb02137.x>
 - [15] Matt Fredrikson, Somesh Jha, and Thomas Ristenpart. 2015. Model Inversion Attacks That Exploit Confidence Information and Basic Countermeasures. In *Proceedings of the 22nd ACM SIGSAC Conference on Computer and Communications Security (CCS '15)*. Association for Computing Machinery, New York, NY, USA, 1322–1333. <https://doi.org/10.1145/2810103.2813677>
 - [16] Karan Ganju, Qi Wang, Wei Yang, Carl A Gunter, and Nikita Borisov. 2018. Property inference attacks on fully connected neural networks using permutation invariant representations. In *Proceedings of the 2018 ACM SIGSAC conference on computer and communications security*. 619–633.
 - [17] Andreas Holzinger, Anna Saranti, Christoph Molnar, Przemyslaw Biecek, and Wojciech Samek. 2022. Explainable AI methods-a brief overview. In *xxAI-Beyond Explainable AI: International Workshop, Held in Conjunction with ICML 2020, July 18, 2020, Vienna, Austria, Revised and Extended Papers*. Springer, 13–38.
 - [18] Matthew Jagielski, Nicholas Carlini, David Berthelot, Alex Kurakin, and Nicolas Papernot. 2020. High Accuracy and High Fidelity Extraction of Neural Networks. In *29th USENIX Security Symposium (USENIX Security 20)*. USENIX Association, 1345–1362. <https://www.usenix.org/conference/usenixsecurity20/presentation/jagielski>
 - [19] Mika Juuti, Sebastian Szlyler, Samuel Marchal, and N. Asokan. 2019. PRADA: Protecting Against DNN Model Stealing Attacks. In *2019 IEEE European Symposium on Security and Privacy (EuroS&P)*. 512–527. <https://doi.org/10.1109/EuroSP.2019.00044>
 - [20] Sanjay Kariyappa and Moinuddin K Qureshi. 2020. Defending against model stealing attacks with adaptive misinformation. In *Proceedings of the IEEE/CVF Conference on Computer Vision and Pattern Recognition*. 770–778.
 - [21] Been Kim, Martin Wattenberg, Justin Gilmer, Carrie Cai, James Wexler, Fernanda Viegas, et al. 2018. Interpretability beyond feature attribution: Quantitative testing with concept activation vectors (tcav). In *International conference on machine learning*. PMLR, 2668–2677.
 - [22] Dieter-Jan Kindermans, Kristof T Schütt, Maximilian Alber, Klaus-Robert Müller, Dumitru Erhan, Been Kim, and Sven Dähne. 2017. Learning how to explain neural networks: Patternnet and patternattribution. *arXiv preprint arXiv:1705.05598* (2017).
 - [23] Zheng Li and Yang Zhang. 2021. Membership Leakage in Label-Only Exposures. In *Proceedings of the 2021 ACM SIGSAC Conference on Computer and Communications Security (CCS '21)*. Association for Computing Machinery, New York, NY, USA, 880–895. <https://doi.org/10.1145/3460120.3484575>
 - [24] Daniel Lowd and Christopher Meek. 2005. Adversarial learning. In *Proceedings of the eleventh ACM SIGKDD international conference on Knowledge discovery in data mining*. 641–647.
 - [25] Nils Lukas, Yuxuan Zhang, and Florian Kerschbaum. 2019. Deep Neural Network Fingerprinting by Conferrable Adversarial Examples. *CoRR abs/1912.00888* (2019). [arXiv:1912.00888](https://arxiv.org/abs/1912.00888) <http://arxiv.org/abs/1912.00888>
 - [26] Scott M. Lundberg and Su-In Lee. 2017. A Unified Approach to Interpreting Model Predictions. In *Proceedings of the 31st International Conference on Neural Information Processing Systems (NIPS'17)*. Curran Associates Inc., Red Hook, NY, USA, 4768–4777.
 - [27] Smitha Milli, Ludwig Schmidt, Anca D. Dragan, and Moritz Hardt. 2018. Model Reconstruction from Model Explanations. (2018). [arXiv:stat.ML/1807.05185](https://arxiv.org/abs/1807.05185)
 - [28] Smitha Milli, Ludwig Schmidt, Anca D. Dragan, and Moritz Hardt. 2019. Model Reconstruction from Model Explanations. In *Proceedings of the Conference on Fairness, Accountability, and Transparency (FAT'19)*. Association for Computing Machinery, New York, NY, USA, 1–9. <https://doi.org/10.1145/3287560.3287562>
 - [29] Takayuki Miura, Satoshi Hasegawa, and Toshiki Shibahara. 2021. MEGEX: Data-Free Model Extraction Attack against Gradient-Based Explainable AI. *CoRR abs/2107.08909* (2021). [arXiv:2107.08909](https://arxiv.org/abs/2107.08909) <https://arxiv.org/abs/2107.08909>
 - [30] Atharva Ingle N Nithin Srivatsav, Swathi N Shayana. 2020. Crop Recommendation Dataset. (2020). <https://www.kaggle.com/datasets/atharvaingle/crop-recommendation-dataset>
 - [31] Tribhuvanesh Orekondy, Bernt Schiele, and Mario Fritz. 2019. Knockoff nets: Stealing functionality of black-box models. In *Proceedings of the IEEE/CVF conference on computer vision and pattern recognition*. 4954–4963.
 - [32] Guillermo Owen. 2013. *Game theory*. Emerald Group Publishing.
 - [33] Nicolas Papernot, Patrick McDaniel, and Ian Goodfellow. 2016. Transferability in machine learning: from phenomena to black-box attacks using adversarial samples. *arXiv preprint arXiv:1605.07277* (2016).
 - [34] Nicolas Papernot, Patrick McDaniel, Ian Goodfellow, Somesh Jha, Z. Berkay Celik, and Ananthram Swami. 2017. Practical Black-Box Attacks against Machine Learning. In *Proceedings of the 2017 ACM on Asia Conference on Computer and Communications Security (ASIA CCS '17)*. Association for Computing Machinery, New York, NY, USA, 506–519. <https://doi.org/10.1145/3052973.3053009>
 - [35] F. Pedregosa, G. Varoquaux, A. Gramfort, V. Michel, B. Thirion, O. Grisel, M. Blondel, P. Prettenhofer, R. Weiss, V. Dubourg, J. Vanderplas, A. Passos, D. Cournapeau, M. Brucher, M. Perrot, and E. Duchesnay. 2011. Scikit-learn: Machine Learning in Python. *Journal of Machine Learning Research* 12 (2011), 2825–2830.
 - [36] Marco Tulio Ribeiro. 2016. GitHub - marcotcr/lime: Lime: Explaining the predictions of any machine learning classifier — github.com. <https://github.com/marcotcr/lime>. (2016). [Accessed 02-Apr-2023].
 - [37] Marco Tulio Ribeiro, Sameer Singh, and Carlos Guestrin. 2016. "Why Should I Trust You?": Explaining the Predictions of Any Classifier. In *Proceedings of the 22nd ACM SIGKDD International Conference on Knowledge Discovery and Data Mining (KDD '16)*. Association for Computing Machinery, New York, NY, USA, 1135–1144. <https://doi.org/10.1145/2939672.2939778>
 - [38] Marco Tulio Ribeiro, Sameer Singh, and Carlos Guestrin. 2018. Anchors: High-precision model-agnostic explanations. In *Proceedings of the AAAI conference on artificial intelligence*, Vol. 32.
 - [39] Ahmed Salem, Yang Zhang, Mathias Humbert, Pascal Berrang, Mario Fritz, and Michael Backes. 2018. ML-leaks: Model and data independent membership inference attacks and defenses on machine learning models. *arXiv preprint arXiv:1806.01246* (2018).
 - [40] Lloyd S. Shapley. 1951. *Notes on the N-Person Game - I: Characteristic-Point Solutions of the Four-Person Game*. RAND Corporation, Santa Monica, CA. <https://doi.org/10.7249/RM0656>
 - [41] Yi Shi, Yalin Sagduyu, and Alexander Grushin. 2017. How to steal a machine learning classifier with deep learning. In *2017 IEEE International Symposium on Technologies for Homeland Security (HST)*. 1–5. <https://doi.org/10.1109/THS.2017.7943475>
 - [42] Reza Shokri, Martin Strobel, and Yair Zick. 2021. On the privacy risks of model explanations. In *Proceedings of the 2021 AAAI/ACM Conference on AI, Ethics, and Society*. 231–241.
 - [43] Reza Shokri, Marco Stronati, Congzheng Song, and Vitaly Shmatikov. 2017. Membership inference attacks against machine learning models. In *2017 IEEE symposium on security and privacy (SP)*. IEEE, 3–18.
 - [44] Congzheng Song and Vitaly Shmatikov. 2019. Overlearning reveals sensitive attributes. *arXiv preprint arXiv:1905.11742* (2019).
 - [45] Florian Tramèr, Fan Zhang, Ari Juels, Michael K. Reiter, and Thomas Ristenpart. 2016. Stealing Machine Learning Models via Prediction APIs. In *Proceedings of the 25th USENIX Conference on Security Symposium (SEC'16)*. USENIX Association, USA, 601–618.
 - [46] Jean-Baptiste Truong, Pratyush Maini, Robert J. Walls, and Nicolas Papernot. 2020. Data-Free Model Extraction. *CoRR abs/2011.14779* (2020). [arXiv:2011.14779](https://arxiv.org/abs/2011.14779)

<https://arxiv.org/abs/2011.14779>

- [47] Binghui Wang and Neil Zhenqiang Gong. 2018. Stealing Hyperparameters in Machine Learning. In *2018 IEEE Symposium on Security and Privacy (SP)*. 36–52. <https://doi.org/10.1109/SP.2018.00038>
- [48] Anli Yan, Teng Huang, Lishan Ke, Xiaozhang Liu, Qi Chen, and Changyu Dong. 2023. Explanation leaks: Explanation-guided model extraction attacks. *Information Sciences* 632 (2023), 269–284. <https://doi.org/10.1016/j.ins.2023.03.020>
- [49] Hao Yuan, Jiliang Tang, Xia Hu, and Shuiwang Ji. 2020. Xgmn: Towards model-level explanations of graph neural networks. In *Proceedings of the 26th ACM SIGKDD International Conference on Knowledge Discovery & Data Mining*. 430–438.
- [50] Yuheng Zhang, Ruoxi Jia, Hengzhi Pei, Wenxiao Wang, Bo Li, and Dawn Song. 2020. The secret revealer: Generative model-inversion attacks against deep neural networks. In *Proceedings of the IEEE/CVF conference on computer vision and pattern recognition*. 253–261.
- [51] Xuejun Zhao, Wencan Zhang, Xiaokui Xiao, and Brian Lim. 2021. Exploiting explanations for model inversion attacks. In *Proceedings of the IEEE/CVF international conference on computer vision*. 682–692.
- [52] Luisa M Zintgraf, Taco S Cohen, Tameem Adel, and Max Welling. 2017. Visualizing deep neural network decisions: Prediction difference analysis. *arXiv preprint arXiv:1702.04595* (2017).